

## BEAM ENERGY LOSS TO PARASITIC MODES IN SPEAR II\*

M. A. Allen, J. M. Paterson, J. R. Rees and P. B. Wilson

Stanford Linear Accelerator Center  
Stanford University, Stanford, California 94305Summary

The energy loss due to the excitation of parasitic modes in the SPEAR II rf cavities and vacuum chamber components has been measured by observing the shift in synchronous phase angle as a function of circulating beam current and accelerating cavity voltage. The resulting parasitic mode loss resistance is  $5 \text{ M}\Omega$  at a bunch length of 6.5 cm. The loss resistance varies with bunch length  $\sigma_z$  approximately as  $\exp(-0.3 \sigma_z)$ . If the measured result is compared with reasonable theoretical predictions, we infer that the major portion of the parasitic loss takes place in ring vacuum components rather than in the rf cavities.

Introduction

Excitation of parasitic modes in rf cavities and vacuum chamber components by a tightly-bunched beam can be a source of significant energy loss in high-energy storage rings. Several calculations which estimate the magnitude of this loss have been made. Sands,<sup>1</sup> using an expression based on an optical resonator model of a periodic structure, has estimated a parasitic energy loss of 0.08 MeV per  $\pi$ -mode cell at a circulating current of 100 mA and a bunch length ( $\sigma_z$ ) of 5 cm, using the parameters proposed for the PEP rf structure.<sup>2</sup> Other calculations have been made recently in which the rf structure is approximated either by a series of closed "pill-box" cavities<sup>3</sup> or by a periodic sequence of disks and cylinders.<sup>3,4</sup> The result for a disk-and-cylinder model of the PEP structure is an energy loss of about 0.012 MeV per  $\pi$ -mode cell, again for a current of 100 mA and a bunch length of 5 cm. For a structure 90 cells in length, this estimate and the estimate by Sands give energy losses of 1 MeV and 7.5 MeV respectively. In addition, fields can be excited by the beam in the various vacuum chamber boxes and components around the ring. The parasitic loss to modes in these "incidental" vacuum chamber resonators can well equal or exceed that to higher-order modes in the rf structure itself.

The large spread between the computed values given above for the higher-mode loss to the rf structure, together with the even greater uncertainty in the loss to be expected for the incidental vacuum chamber components, makes it imperative to seek out means for measuring these losses experimentally. Sands and Rees<sup>5</sup> have proposed a method for measuring the loss to a cavity or vacuum chamber box in which a short pulse of current is sent along a thin wire stretched on the axis of the component under test. Initial results<sup>6</sup> are promising, and the method might eventually be refined to the point where each vacuum chamber component can be checked to see whether the level of higher-mode loss is acceptable. We also realized that SPEAR II uses an rf structure similar to that proposed for PEP. In particular, the rf frequency is the same; hence the bunch length and the excitation of parasitic modes in the incidental vacuum chamber components are expected to be similar.

Three methods have been proposed for measuring the parasitic losses in SPEAR II. The first, a direct calorimetric measurement of heating in an idling (non-driven) rf cavity in which the fundamental mode has been tuned far off resonance, has not yet been pursued because it is not compatible with the current SPEAR operating program. It would be worthwhile to make this measurement eventually, because the result would make

it possible to separate the portion of the loss in the rf cavities from the total loss. For the present we have instead pursued two measurement techniques, which rely mainly on the existing SPEAR control room instrumentation supplemented by a few additional simple devices, for obtaining the total parasitic loss to all ring components. In the first approach, the parasitic loss is obtained from a measurement of the net rf power input into the accelerating cavities; in the second, it is obtained by measuring the shift in synchronous phase angle as a function of beam current and peak cavity voltage.

Measurement by Net Cavity Power Input

In this measurement, a single cavity is used to store a beam at 1.5 GeV at a fixed peak voltage so that cavity wall losses remain constant. The power input to the cavity is then measured as a function of stored beam current  $i$ . The higher-mode energy loss per turn is computed from the following expression:

$$V_{hm}(i) = (1/i) [P(i) - P(0)] - V_s - V_{fm}$$

Here,  $P(i)$  is the net (incident minus reflected) power input into the cavity at current  $i$ ,  $P(0)$  is the net power input at zero current,  $eV_s$  is the energy loss per turn due to synchrotron radiation, and  $V_{fm}$  is the loss due to the excitation of the fundamental mode in the idling cavities. In turn,  $V_{fm}$  is obtained by measuring the output from a coupling probe in each idling cavity. The calibration factor for each coupling probe is obtained by measuring either the synchrotron frequency or the quantum lifetime at a relatively high energy (2.5 GeV) and a low beam current, so that the synchrotron radiation loss is dominant over current-dependent losses. The peak cavity voltage  $\hat{V}$  is then readily calculated from the known ring parameters. The voltage  $V_b$  seen by the beam is now obtained from the relation  $V_b/\hat{V} = \hat{V}/V_0 = \cos \psi$ , where  $V_0$  is the peak voltage the cavity would have at resonance and  $\psi$  is the tuning angle. The ratio  $\hat{V}/V_0$  is obtained by observing the change in probe output as the tuners are run to resonance from their (off-resonant) position set during the parasitic loss measurements. In this way, the resistance per cavity for loss to the fundamental mode was measured to be  $V_b/i = 0.5 \text{ M}\Omega$  at  $\cos^2 \psi = -15 \text{ db}$ . The value of this resistance obtained from the cavity parameters, assuming a matched rf source, is  $V_b/i = [R_{sh}/(1 + \beta)] \cos^2 \psi$ , where  $R_{sh}$  is the cavity shunt impedance and  $\beta$  the coupling coefficient. For  $\beta = 1.8$  and  $R_{sh} = 40 \text{ M}\Omega$  (values obtained from cold-test measurements of  $\beta$  and loaded  $Q$  and from an R/Q computed by LALA), a value of  $V_b/i = 0.48 \text{ M}\Omega$  is calculated, in good agreement with the measured result.

Values of  $R_{hm} = V_{hm}/i$ , obtained at high circulating currents where the change in net input power is largest and the best accuracy is to be expected, were  $4.5 \text{ M}\Omega$  at 800 kV and 25 mA and  $3.4 \text{ M}\Omega$  at 1120 kV and 40 mA. These results can be compared with Sands' estimate,<sup>1</sup> scaled to SPEAR, of  $4.1 \text{ M}\Omega$  for the higher-mode loss into the three rf cavities present in the ring at the time of the measurement. Although there is good agreement between this theoretical value and the measured results at high circulating currents, considerably lower higher-mode loss resistances were measured at lower currents. Since the bunch length is shorter at lower currents, higher resistances would in fact be expected. Because of this inconsistency, and because of the many pitfalls associated with making precise rf power measurements, it was decided to concentrate

\*Work supported by the U. S. Energy Research and Development Administration.

further effort on the synchronous phase shift method for measuring the parasitic loss.

### Measurement by Shift in Synchronous Phase

The synchronous phase angle, measured from the crest of the rf cavity voltage, is given by

$$\cos \phi = \frac{V_s + iR}{\hat{V}} \quad (1)$$

As discussed previously, we expect the total loading resistance  $R$  to be the sum of a component giving the loss to the fundamental mode in the idling cavities, and a component which gives the loss to the parasitic modes. Furthermore, we expect<sup>1,3,4</sup> the higher-mode component to depend strongly on bunch length, which in turn depends on both beam current and peak rf voltage. Thus,  $R = R_{fm} + R_{hm}(\hat{V}, i)$  and we expect to see a shift in synchronous phase as beam current is varied at constant peak voltage, and as peak voltage is varied at constant beam current. Using data taken under these two conditions, together with measurements of bunch length,  $\sigma_z(\hat{V}, i)$ , we might hope to unravel the dependence of  $R_{hm}$  on bunch length in SPEAR II.

A shift in synchronous phase could in principle be detected by making an accurate measurement of the shift in time at which the bunch passes a fixed point, such as a beam position monitor electrode. At an rf frequency of 358 MHz, a  $1^\circ$  phase shift corresponds to a time shift of only 8 picoseconds, a difficult measurement to make at best. It is possible, however, to measure a  $1^\circ$  phase shift between two sine waves at 358 MHz. An instrument which can compare the phase of two signals to this accuracy at this frequency is the Rf Vector Voltmeter.<sup>7</sup> If one input to the Vector Voltmeter is obtained from the rf cavity used to store the beam, and if the second input is a signal having a phase determined by the passage of the bunch by a pickup electrode, the instrument will measure the shift in synchronous phase as either  $\hat{V}$  or  $i$  is varied. A diagram of the experimental arrangement is given in Fig. 1.

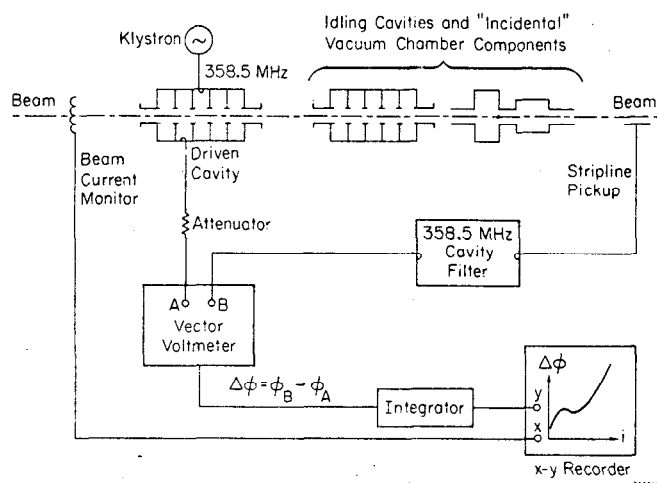


Fig. 1--Instrumentation for measuring shift in synchronous phase.

The chief difficulty in this method of measurement is the necessity for converting the signal induced by the beam on the pickup electrode into a semblance of a sine wave that will be acceptable to the Vector Voltmeter. This processing is accomplished by a transmission cavity having a  $Q$  sufficiently high so that the filling time is comparable to the time between the passage of successive bunches. Alternatively, since the frequency spectrum of the signal from such a pickup electrode is composed of a series of harmonics of the

revolution frequency, the cavity can be considered as a filter which rejects all components except the harmonic at the rf frequency. A transmission cavity with a suitable  $Q$  was constructed from a half-wavelength section of standard 3-1/8" copper coaxial transmission line. The loaded  $Q$  of the cavity was measured to be 1500 with the two coupling loops adjusted to have coupling coefficients close to unity. Although the loaded  $Q$  could have been made higher (the unloaded  $Q$  of the cavity was 4400), the phase shift across the cavity would have been more sensitive to temperature changes. In the present design, a  $0.4^\circ\text{C}$  temperature change results in a phase shift of  $1^\circ$ .

The accuracy of the apparatus was checked by measuring the phase shift as a function of peak cavity voltage at low current and 2.5 GeV, such that  $V_s \gg iR$ . The measured and calculated values of phase shift were in good agreement.

Data on the shift in synchronous phase as a function of beam current at constant cavity voltage are given in Fig. 2. Since the instrument does not measure absolute values of phase but only relative changes in phase, the phase scale on the vertical axis has been determined by fitting the data in ways which will be described later. As will be seen, this calibration might be off by a degree or two. A further caveat is that these curves are not to be trusted in fine detail ( $\pm 1/2^\circ$ ) and, especially, they are likely to be misleading below currents of several milliamperes where the Vector Voltmeter produces a phase shift error which increases rapidly as the amplitude of the excitation on the channel (Channel B) coming from the beam pickup is decreased. The curves shown in Fig. 2 are the average between two runs in which this systematic shift in phase as a function of beam current is in opposite directions.

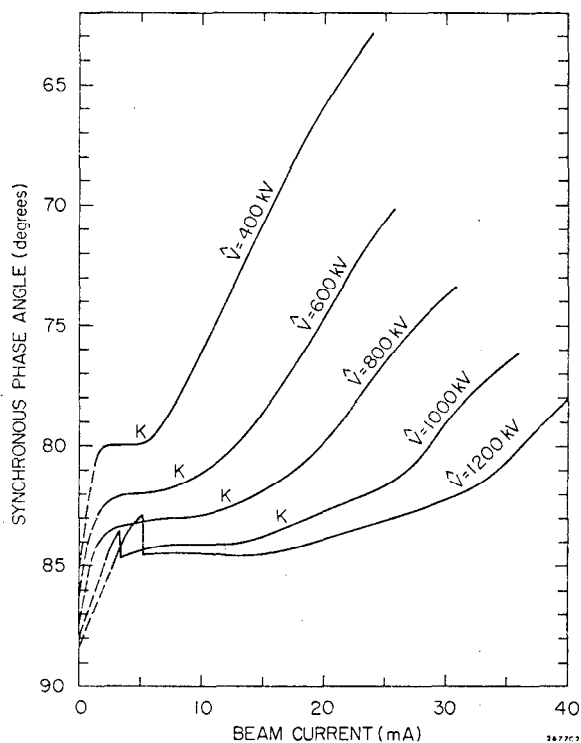


Fig. 2--Synchronous phase as a function of beam current at constant peak cavity voltage at 1.5 GeV.

If the higher-mode resistance  $R_{hm}$  were a constant, a phase shift plot such as that in Fig. 2 would consist of more or less straight lines having intercepts on the vertical axis given by  $\phi(0) = \cos^{-1}(V_s/\hat{V})$ . The fact that the curves are nowhere near linear is a reflection of the fact that rapid changes in bunch length take

place as a function of current and voltage. To interpret these phase plots, we must know the dependence of bunch length on  $i$  and  $\hat{V}$ . The experimentally-measured dependence is shown in Fig. 3. Note the following features of these curves, which will be used in interpreting the phase shift data. At 400 kV the bunch length is nearly constant as a function of current above about 10 mA. At about 20 mA the bunch length is nearly the same for all cavity voltages from 400 to 1000 kV. At 25 mA and above  $\sigma_z$  (1000 kV) tends to be greater than  $\sigma_z$  (400 kV), while at 20 mA  $\sigma_z$  decreases monotonically with increasing  $\hat{V}$ . Finally, the knee in each curve, where slope is varying most rapidly, shifts to progressively higher currents as  $\hat{V}$  is increased. In Fig. 2, the locations of these knees are indicated by K's. We see that these also mark approximately the locations of knees in the phase shift plots.

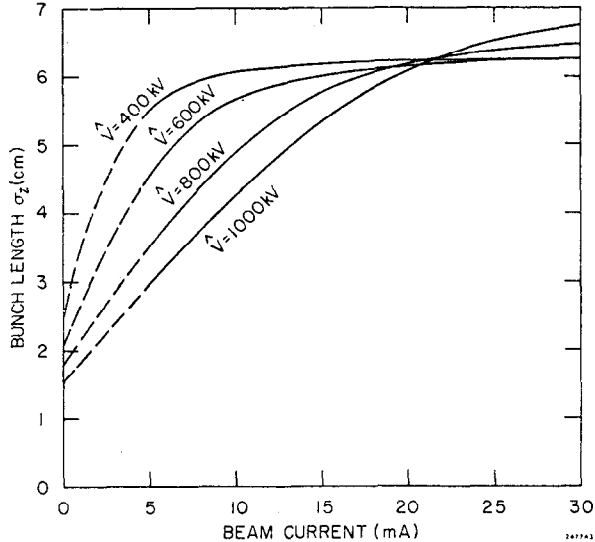


Fig. 3--Bunch length as a function of beam current for several values of peak cavity voltage at 1.5 GeV.

An additional feature of interest in the phase plots of Fig. 2 are the abrupt jumps in phase, indicating discontinuous changes in bunch length, at about 5 mA on both the 1000 kV and 1200 kV curves. Discontinuous changes in both bunch length and beam width were indeed observed directly by measurements made just above and just below the currents indicated by the phase jumps. The beam is also vertically unstable at currents just above the phase jumps. In addition, there is an abrupt increase in the strength of the beam excitation at the synchrotron frequency as the current increases through the phase jump. A possible interpretation of these phase jumps is that they mark regions of negative resistance on the  $\phi(i)$  curves, such that an increase in current would produce a decrease in loss if it were not for the jumps. A stable bunch length is not possible in a region where  $d\phi/di$  is positive.

We can extract a parasitic mode resistance from the data given in Fig. 2 from the slope of the 400-kV curve above 10 mA, where the bunch length is nearly constant at about 6.5 cm. By differentiating Eq. (1) with respect to current, we find

$$R = \hat{V} \sin \phi (-d\phi/di) - i(dR/di) \quad (2)$$

If bunch length is independent of current, we can set  $dR/di = 0$  and  $R$  can then be calculated from the slope  $d\phi/di$  at constant voltage. An error of a few degrees in the absolute value of  $\phi$  makes little difference, since  $\sin \phi \approx 1$ . In this manner, we obtain  $R = 6.8 \text{ M}\Omega$  in the 10 - 15 mA region of the 400-kV curve. We next

look at the error that is made by ignoring a small rate of change of bunch length with current. Let us approximate the higher-mode loss by  $R_{hm} \approx A \exp(-B\sigma_z)$ . That this is a reasonable form for the higher-mode loss (over the limited range of bunch lengths under consideration here) is shown by the detailed calculations in Refs. 3 and 4. We will later show that experimentally  $B \approx 0.3$  for SPEAR II. Using this form for  $R_{hm}$  in Eq. (2), we obtain

$$\Delta R/R = iB(1 - R_{fm}/R)(d\sigma_z/di) \quad ,$$

where  $\Delta R = i(dR/di)$ . For  $B = 0.3$ ,  $i = 20 \text{ mA}$ ,  $R_{fm} = 1.5 \text{ M}\Omega$  and  $R \approx 6$ , we calculate that a  $d\sigma_z/di$  of 1 cm per 50 mA will produce a 10% error in  $R$ . This is the order of the slope of the 400-kV curve as drawn in Fig. 3, and is below the resolution of the actual bunch length data. The sign of the error is such that the true value of  $R$  will be larger than the value calculated from Eq. (2) under the assumption that  $dR/di = 0$ .

The change in synchronous phase was also measured as a function of cavity voltage at constant current. This data is analyzed by assuming an absolute value of phase at some particular voltage, say 1200 kV, and then using the measured phase shifts to obtain the phases at other voltages. The loss resistance  $R$  is then computed from Eq. (1). The characteristics discussed previously of the  $\sigma_z(\hat{V}, i)$  curves are used to determine the best value of  $\phi(1200 \text{ kV})$ . When we have chosen the correct absolute phase, we should find, for example, that at 20 mA  $R$  is nearly constant independent of  $\hat{V}$ , since the bunch length is also nearly constant. Results are given in Table I for several different values of the absolute phase at 1200 kV. We see that a phase at 1200 kV of  $81^\circ$  or  $82^\circ$  produces a roughly constant value of  $R$  over the measured values of  $\hat{V}$ , while there is considerable variation in  $R$  for  $80^\circ$  and  $83^\circ$ . Proceeding in a similar manner for other values of beam current, we obtain the results shown in Table II. The phases have been chosen such that  $R$  is roughly constant at 400 kV, while at 1200 kV the variation in  $R$  is consistent with the bunch length data shown.

TABLE I.

$R$  as a function of  $\hat{V}$  at 20 mA  
for several assumed values of phase at 1200 kV

| $\hat{V}$ | $\phi$     | $R$            | $\phi$     | $R$            | $\phi$     | $R$            | $\phi$     | $R$            |
|-----------|------------|----------------|------------|----------------|------------|----------------|------------|----------------|
| 1200      | $80^\circ$ | 8.7 M $\Omega$ | $81^\circ$ | 7.6 M $\Omega$ | $82^\circ$ | 6.6 M $\Omega$ | $83^\circ$ | 5.6 M $\Omega$ |
| 1100      | 79.6       | 8.2            | 80.6       | 7.2            | 81.6       | 6.3            | 82.6       | 5.3            |
| 1000      | 79.0       | 7.8            | 80.0       | 6.9            | 81.0       | 6.1            | 82.0       | 5.2            |
| 900       | 78.0       | 7.6            | 79.0       | 6.8            | 80.0       | 6.1            | 81.0       | 5.3            |
| 800       | 76.7       | 7.5            | 77.7       | 6.8            | 78.7       | 6.1            | 79.7       | 5.4            |
| 700       | 74.2       | 7.8            | 75.2       | 7.2            | 76.2       | 6.6            | 77.2       | 6.0            |
| 600       | 71.5       | 7.8            | 72.5       | 7.3            | 73.5       | 6.8            | 74.5       | 6.3            |
| 500       | 68.3       | 7.5            | 69.3       | 7.1            | 70.3       | 6.7            | 71.3       | 6.3            |
| 450       | 66.3       | 7.3            | 67.3       | 6.9            | 68.3       | 6.6            | 69.3       | 6.2            |
| 400       | 63.3       | 7.2            | 64.3       | 6.9            | 65.3       | 6.6            | 66.3       | 6.3            |

The data in Fig. 2 can also be converted into resistances using Eq. (1). The result is shown in Fig. 4 for three values of  $\phi_0$ , where  $\phi_0$  is a phase deviation which is added to the scale shown on the vertical axis of Fig. 2. A value of  $\phi_0 = -2^\circ$  is seen to be most consistent with the bunch length data. That is,  $R(400 \text{ kV})$  decreases monotonically with increasing current, all the curves cross in the neighborhood of 20 mA and the curve for  $R(1200 \text{ kV})$  continues to decrease above 20 mA. For  $\phi_0 = -2^\circ$ , the values of  $\phi(1200 \text{ kV})$  at currents of 10, 15, 20 and 25 mA are  $82.5^\circ$ ,  $82.5^\circ$ ,

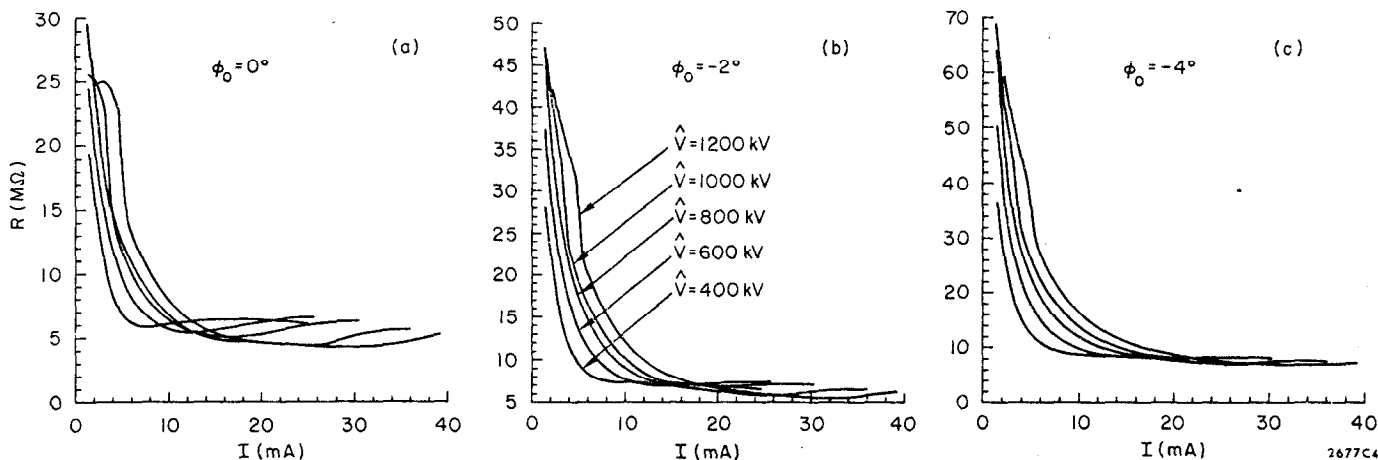


Fig. 4--Total loading resistance computed from  $R = (1/i)[\hat{V} \cos(\phi + \phi_0) - V_s]$ , where  $\phi$  is the phase as shown in Fig. 2 and  $\phi_0$  is a phase offset.

TABLE II.

Best choice of  $\phi$  (1200 kV)  
to give R consistent with bunch length data

| Current | $\phi$ (1200 kV) | R (400 kV) | $\sigma_z$ (400 kV) | R (1200 kV) | $\sigma_z$ (1200 kV) |
|---------|------------------|------------|---------------------|-------------|----------------------|
| 25.0 mA | 80.5°            | 6.1 MΩ     | 6.4 cm              | 6.1 MΩ      | 6.6 cm               |
| 20.0    | 81.5             | 6.7        | 6.3                 | 6.5         | 6.3                  |
| 15.5    | 82.5             | 6.9        | 6.3                 | 7.1         | 5.5                  |
| 10.2    | 83.0             | 6.8        | 6.2                 | 10.7        | 4.6                  |

82° and 81°, respectively. These values agree well with those given in Table II, obtained from the phase variation measured at constant voltage. Finally, from Fig. 4b we see that, at 20 mA where  $\sigma_z \approx 6.3$  cm, the total loss resistance R is about 7 MΩ. This result is also in reasonable agreement with the results in Table II.

We are now in a position to make an estimate of the variation of parasitic loss with bunch length. Higher-mode loss resistances  $R_{hm} = R - 1.5 \text{ M}\Omega$  are obtained for the various cavity voltages in Fig. 4b at a current of 10 mA. In Fig. 5 these resistances are plotted as a function of the measured bunch length for the corresponding cavity voltages at this current. The plotted results are also seen to be in agreement with the values of R and  $\sigma_z$  given in the last two columns of Table II. It is seen that the variation of  $R_{hm}$  with bunch length is slower than that computed<sup>4</sup> for the rf cavities alone, and that the magnitude is considerably higher. Recall also that the analysis from  $d\phi/di$  at constant voltage gave a value of  $R_{hm} = 5.3 \text{ M}\Omega$  at 400 kV and 15 mA ( $\sigma_z \approx 6.3$  cm). From Table II we have about the same result from the analysis at constant current. This combined result is plotted as an open circle in Fig. 5. Also shown is the value estimated by Sands.

#### Implications for High Energy Rings

If the result of the present measurement ( $R_{hm} \approx 5 \text{ M}\Omega$  at  $\sigma_z = 6.5$  cm) is scaled from SPEAR II to PEP parameters assuming first that all of the higher-mode loss occurs in the rf cavities, then  $R_{hm}$  scales as  $nL/b$  where n is the total number of individual cells in the rf structure, L is the circumference of the ring (proportional to the harmonic number for a fixed rf frequency) and b is the number of bunches. Thus, for a 90-cell PEP structure,  $R_{hm}(\text{PEP}) = (90/20)(2592/280)(1/3) \times 5 \text{ M}\Omega = 70 \text{ M}\Omega$ . In the design

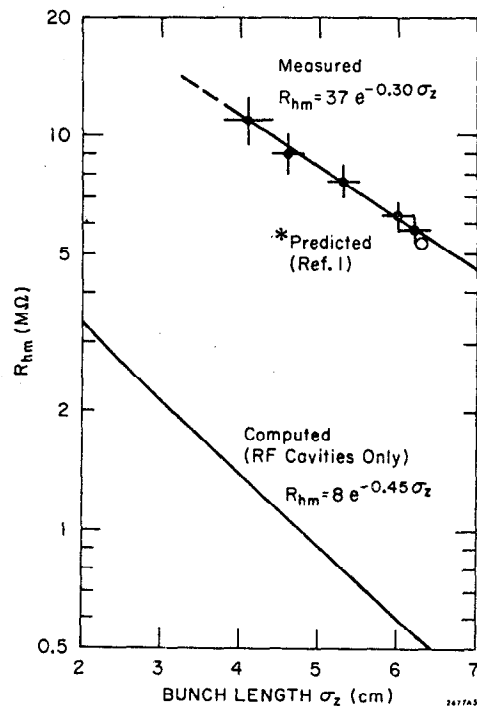


Fig. 5--Computed and measured parasitic mode loss resistances as a function of bunch length.

of the PEP rf system, excess rf power has been provided to allow for a 75-MΩ parasitic loss resistance.

On the other hand, we have seen that the present experimental results give a value for the parasitic loss which is nearly an order of magnitude greater than the loss predicted by recent computations for the rf cavities alone. It is about three times higher than the loss computed assuming that the rf structure is composed entirely of pill-box cavities with no beam apertures. It is difficult to see how the loss in a structure with a beam aperture can be larger than that for a closed pill-box cavity, where the calculation is not approximate. We are compelled to conclude that either the present measurement is in error, or that a major fraction of the higher-mode loss occurs in the vacuum chamber components outside of the rf cavities. If we assume as a worst case that all of the parasitic loss occurs in the vacuum chamber components, and that the PEP and SPEAR components will have similar loss characteristics per unit length of ring circumference, then

$R_{\text{hm}}$  scales as  $L^2/b$  and  $R_{\text{hm}}(\text{PEP}) = (2592/280)^2(1/3) \times 5 \text{ M}\Omega = 140 \text{ M}\Omega$ .

No great care was taken in the design of the SPEAR vacuum chamber components to minimize higher-mode loss, and it therefore seems reasonable that by careful attention to the design of the PEP components the average loss per unit length can be reduced by a factor of two to reduce the total parasitic loss resistance to the acceptable value of  $75 \text{ M}\Omega$ . In any event, the present measurements indicate that parasitic mode loss must be an important consideration in the design of the vacuum chamber components for the next generation of electron-positron storage rings.

#### Acknowledgements

The authors wish to thank K. L. F. Bane for producing the computer-generated plots given in Fig. 4. We express our appreciation also to J. B. Styles for designing and constructing the cavity filter used in these measurements.

#### References

1. M. Sands, PEP-90, July 1974 (unpublished).
2. M. A. Allen and P. B. Wilson, Proc. of the 9th Int. Conf. on High Energy Accel. (SLAC, May 1974), p. 92.
3. E. Keil, C. Pellegrini, A. Turrin and A. Sessler, to be published in Nucl. Inst. and Meth.
4. K. Bane and P. Wilson, PEP-112, March 1975 (unpublished).
5. M. Sands and J. Rees, PEP-95, August 1974 (unpublished)
6. E. Hartwig, LBL. Private communication.
7. Hewlett-Packard Model 8405 A.